

New approach for Ductility analysis of partially prestressed concrete girders

Jure Radnić¹, Radoslav Markić², Nikola Grgić^{*3} and Dragan Ćubela⁴

¹Department of Concrete Structures and Bridges, Faculty of Civil Engineering, Architecture and Geodesy, University of Split, Matice Hrvatske 21000 Split, Croatia

²Department for Mechanics, Materials and Construction, Faculty of Civil Engineering, University of Mostar, Matice hrvatske b.b. Mostar, Bosnia and Herzegovina

³Department of Concrete Structures and Bridges, Faculty of Civil Engineering, Architecture and Geodesy, University of Split, Matice Hrvatske 21000 Split, Croatia

⁴Department for Mechanics, Materials and Construction, Faculty of Civil Engineering, University of Mostar, Matice hrvatske b.b. Mostar, Bosnia and Herzegovina

(Received November 1, 2018, Revised February 14, 2019, Accepted February 20, 2019)

Abstract. Expressions for the calculation of ductility index for concrete girders with different ratios of prestressed and classical reinforcement were proposed using load–displacement, load–strain and load–curvature relation. The results of previous experimental static tests of several large-scale concrete girders with different ratio of prestressed and classical reinforcement are briefly presented. Using the proposed expressions, various ductility index of tested girders were calculated and discussed. It was concluded that the ductility of girders decreases approximately linearly by increasing the degree of prestressing. The study presents an expression for the calculation of the average ductility index of classical and prestressed reinforced concrete girders, which are similar to the analysed experimental test girders.

Keywords: concrete; prestressed girders; ductility index; experimental test; analytical expression; load-displacement relation, load-strain relation; load-curvature relation

1. Introduction

The behaviour of structures exposed to static and dynamic loads is well-characterised by their ductility. In general, ductility is a measure of nonlinear behaviour of the structure. It can be defined as a feature of the structure that can submit nonlinear deformations before failure. Significant nonlinearity occurring in ductile structures causes softening and slow pronounced failure Fig. 1.

The failure of brittle structures is fast and explosive, in the absence of previous nonlinearities. It is preferred that all structures in practice are sufficiently ductile. Ductility enables the redistribution of internal forces in statically indeterminate structures and reduces induced seismic forces in the structure due to their softening and dissipation of accumulated internal energy.

An exact mathematical definition and method for quantifying structure ductility has not yet to be fully agreed upon. Typically, it is defined through displacement (u), adsorbed energy (E) and curvature (φ), which correspond to displacement ductility, energy ductility and curvature ductility (Fig. 2). Also, terms deformation ductility and rotation ductility were used. The dimensionless ductility factor (coefficient) is commonly used as a measure of structure ductility. It is usually defined as the ratio of the abovementioned structure features at maximum load F_m that

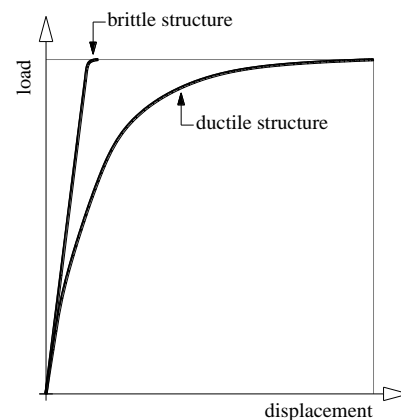


Fig. 1 Brittle and ductile structures

cause u_m , E_m , φ_m , and features at load F_n that cause some nonlinearity u_n , E_n , φ_n . Therefore, these differently expressed ductility factors are interconnected. Namely, the accumulated energy is defined as the area under the load (F)-displacement (u) curve, and the curvature is also directly related to displacements.

Precise calculation of the structure ductility is very complex because it depends on many parameters, such as type and rigidity of structure, material parameters, cross-sectional parameters, reinforcement design, prestressing, and loading type. Many experimental and analytical studies have been carried out within recent decades regarding displacement ductility, energy ductility and curvature ductility of classically reinforced and prestressed concrete

*Corresponding author, Assistant Professor
E-mail: nikola.grgic@gradst.hr

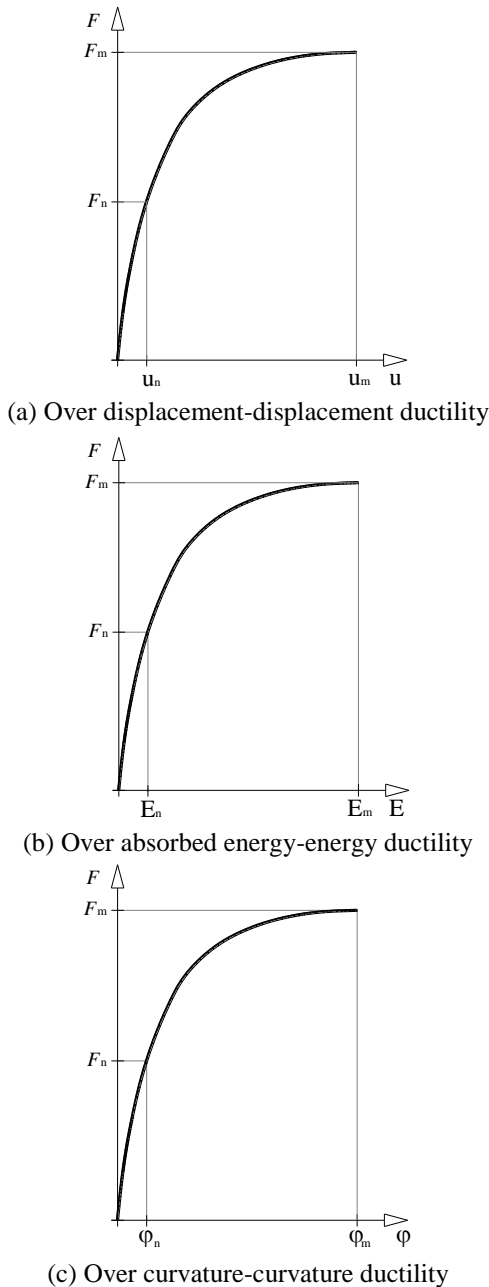


Fig. 2 Most common approaches to calculation of ductility

members. Some of the literature that discusses these issues is presented below.

Park and Paulay (1975) suggested that the curvature ductility index is the ratio of curvature at the ultimate stage to the curvature when the tension steel first yields. Park (1989) discussed definition for the required and available ductility used in seismic design of concrete structures. Abdelrahmen *et al.* (1995) presented displacement ductility index as a ratio of displacement at failure and the equivalent displacement of the uncracked section at a load equal to the ultimate load. Naaman and Jeong (1995) suggested a new expression of the energy ductility index. Hofstetter and Mang (1996) presented a paper summarising a survey of computational mechanics of reinforced and prestressed concrete structures. They noted important parameters and

their complexity that affected the calculations and results. Spadea *et al.* (1997) presented the energy ductility factor as the ratio of total energy to the energy up to 75% of the ultimate load. Grace *et al.* (1998) used the ratio of inelastic energy to the total energy to quantify the energy ductility of FRP reinforced beams. Pisant and Regan (1998) examined the possible demands for ductility, allowing for redistribution of moments in linear reinforced concrete elements. The tests included series of beam tests and slab test with respective slenderness ratios; thus one important aspect of the size effect was investigated. Pam *et al.* (2001) proposed analytical method that takes into account the stress-path dependence of the constitutive properties of the materials. Presented study deals with the post-peak behaviour and flexural ductility of doubly reinforced normal and high strength concrete beam sections. Dolan *et al.* (2001) defined the curvature ductility of beams with FRP tendons as the ratio of the curvature at failure to the curvature at service load. Zou (2003) defined the displacement ductility factor of fibre reinforced polymer prestressed concrete beams as the ratio of deflection at failure to the deflection at first cracking, multiplied by the ratio of the ultimate load to the cracking load. Thomsen *et al.* (2004) investigated uses of fibre reinforced polymer (FRP) in strengthening of RC beams and the effects of this strengthening technique on the response and failure modes of a reference RC beam. In the article they defined the energy ductility as the ratio between the energy of the system at failure and the energy of the system at first steel yield. Tan *et al.* (2005) defined the displacement ductility factor as the ratio of the displacement at 95% peak load and the displacement at 67% peak load. Yang *et al.* (2008) experimentally investigated the ductility of high strength concrete beams. In the article, the researchers defined ductility index as the ratio of ultimate displacement at beam failure and displacement at yielding of tensile reinforcement. For the computation of the ductility index they calculated the point of yield displacement from the equivalent elasticity-plasticity relationship of secant elastic stiffness at 75% of the maximum load-displacement curve and the ultimate displacement at the point of 80% of the maximum load after the maximum (peak) load. Also the effect of concrete compressive strength, web reinforcement ratio, tension ratio and shear span to beam depth ratio on ductility were investigated. Mari *et al.* (2011) investigated the response of fibre reinforced polymer (FRP) strengthened concrete structures in flexure using a nonlinear and time-dependent evolutive analysis model, previously developed by the authors. The model shows generally good agreement between the theoretical and the experimental results of all tested beams and enables prediction of adequate failure mode of structure. Arslan (2012) explored the effects of seismic code parameters for columns and beam sections on the ductility of the section and load bearing system on an RC frame. Curvature ductility in RC sections and displacement ductility values in the frame system were calculated according to the axial load level on the columns, the longitudinal reinforcement ratio, concrete compression strength and the transverse strength of parameters. These values are calculated by changing

parameters, such as the transverse reinforcement, compression bar ratio and the concrete compression strength for beams. Ghallab (2014) first summarised the known calculation methods of the ductility of structural members. An experimental study was performed to investigate the effect of several variables on the ductility of reinforced continuous concrete beams externally strengthened using Parafil rope. Test results showed that the ductility of the externally prestressed concrete beams was significantly reduced due to prestressing. Bouzid and Kassoul (2016) presented approach to evaluate the curvature ductility factor of high strength concrete beams according to Eurocode 2 (EN 1992-1-1 2004). They was conducted a parametric study on the factors influencing the curvature ductility of inflected sections. Proposed formula allows calculating the curvature ductility factor of high strength concrete beams directly according to the concrete strength, the yield strength of steel and the ratio of tension and compression reinforcements. Chen *et al.* (2017) proposed a strategy for flexural ductility design of RC beams taking into account confinement. This study deals with the confinement for desirable flexural ductility performance of both normal and high strength concrete beams.

First, this paper presents one approach and proposes expressions for calculation of the ductility index of classically reinforced and prestressed concrete girders with internal pre-tensioned tendons (wires), subjected to static load. The proposed expressions are based on load-displacement, load-strain and load-curvature relations. Then, results from previously tested large-scale concrete girders with different ratios of prestressed and classical reinforcement are briefly presented. According to the previously proposed expressions, displacement ductility index, strain ductility index (separately for concrete, classical and prestressed reinforcement) and curvature ductility index are calculated for all tested girders. The effect of degree of prestressing and type of tested girders on their ductility was discussed. The expression for calculation of the average ductility index for classically reinforced and prestressed concrete girders as analysed experimental girders is proposed. Main conclusions of research are presented at the end of the paper.

2. Proposed approach for calculation of structure ductility

2.1 Calculation of ductility over load-displacement relation

The adopted approach for calculation of the structure ductility index of classically reinforced and prestressed concrete girders defined by load (F)-displacement (u) relationship is presented in Fig. 3. Displacement ductility index (c_{du}) is calculated according to following expression

$$c_{du} = [(u_m - u_n)/(u_m - u_o)] \cdot [(F_m - F_n)/F_m] \quad (1)$$

where u_m is a displacement at ultimate bearing capacity of the girder, u_n is a displacement at specified nonlinearity in

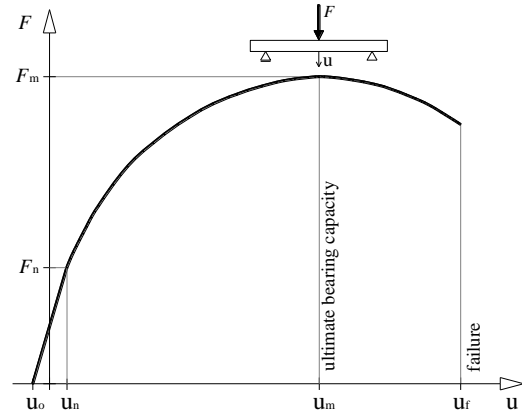


Fig. 3 Schematic presentation of load (F)-displacement (u) relation

the girder, u_o is an initial displacement due to prestressing, F_m is a maximum load and F_n is a load at beginning of a specified nonlinearity. Displacement at structure failure u_f was not considered because the accuracy of the load-displacement relation after reaching u_m was questionable. Namely, the path of the load-displacement curve depends on several parameters, such as loading rate, accuracy of testing equipment, and size of test sample. From eq. (1) it is clear that the value of the displacement ductility index is in following range

$$0 \leq c_{du} \leq 1 \quad (2)$$

The ductility index $c_{du}=0$ corresponds to the ideal brittle structures. A ductility index of $c_{du}=1$ corresponds to the ideal ductile structures where the first nonlinearities occurred in $F_n=0$. Not taking into consideration the displacement larger than u_m , smaller values for c_{du} were obtained.

The first factor on the right side in Eq. (1) includes the effect of differences in displacement at maximum load and displacement at specified nonlinearity in the concrete girder. The second factor includes the effect of differences in maximum load and load that produces the specified nonlinearity in the concrete girder. Namely, it includes the effect of the remaining (reserve) load capacity after reaching F_n . According to Fig. 3, by comparing the load-displacement relationship for two different concrete structures with equal values of u_o , u_n , u_m , F_m and different values of F_n (F_{n1}, F_{n2} where $F_{n1} > F_{n2}$), it can be concluded that a structure with F_{n2} has a greater displacement ductility index than a structure with F_{n1} , i.e., $(F_m - F_{n2}) > (F_m - F_{n1})$. From Eq. (1) and Fig. 3 it is also clear that $c_{du} \rightarrow 0$ if $(F_m - F_n) \rightarrow 0$. That correspondence to the elastic-ideal brittle and elastic-ideal plastic behavior of the concrete girder.

The adopted value of F_n directly affects c_{du} . Generally, F_n should correspond to appearances of certain nonlinearities in the structure. It is logical to take a load F_n that causes the appearance of the first nonlinearities in the concrete structure. The first nonlinearity is usually associated with the appearance of cracks in the concrete tensile zone after exceeding the limit tensile strain (stress) of concrete. Next, the structure stiffness suddenly falls and increases its displacements, as well as the strains (stresses)

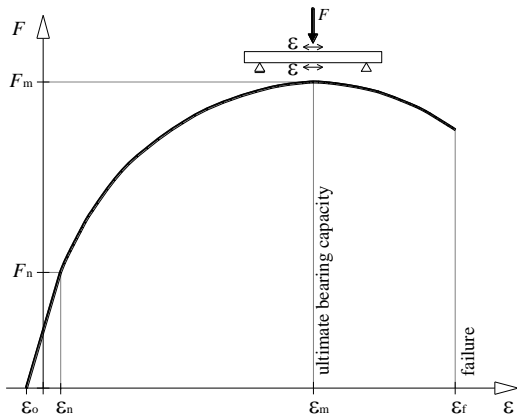


Fig. 4 Schematic presentation of load (F)-strain (ε) relation

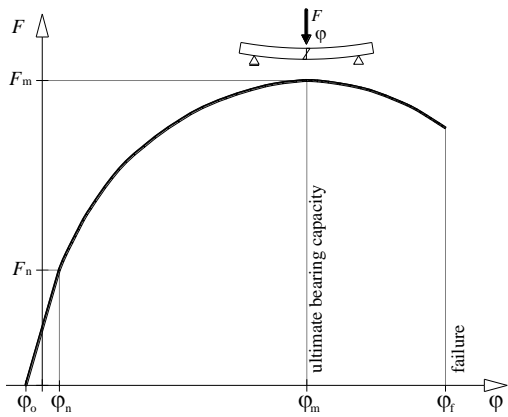


Fig. 5 Schematic presentation of load (F)-curvature (φ) relation

in the classical reinforcement, prestressed reinforcement and compression concrete. Therefore, it is logical to adopt $u_n = u_{cr}$ and $F_n = F_{cr}$, where u_{cr} , F_{cr} are the displacement and loading at the appearance of concrete cracks.

In concrete structures with a small cross-sectional compressive area of concrete, initial structure nonlinearities are related to the occurrence of concrete yielding in compression. In that case adopted u_n , F_n should correspond to such a state.

In a prestressed concrete girder with high strains (stresses) in the tendons, initial nonlinear behaviour can occur due to yielding of prestressed reinforcement. Next, u_n , F_n should represent such a state. In a girder with small compressive flange width with higher lateral slenderness, less lateral stability and brittle behaviour may occur even for service loads.

2.2 Calculation of ductility over load-strain relation

Analogously to approach presented in section 2.1, the structure ductility index can be calculated on the basis of the load (F)-strain (ε) relationship (Fig. 4) by

$$c_{de} = [(\epsilon_m - \epsilon_n) / (\epsilon_m - \epsilon_o)] \cdot [(F_m - F_n) / F_m] \quad (3)$$

where c_{de} is the strain ductility index, ϵ_m is the strain of some material of girder that correspond to maximum load, ϵ_n is the strain at specified nonlinearity in that material, ϵ_o is

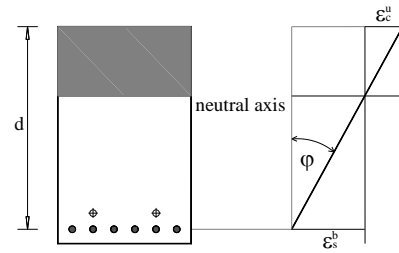


Fig. 6 Cross-section curvature

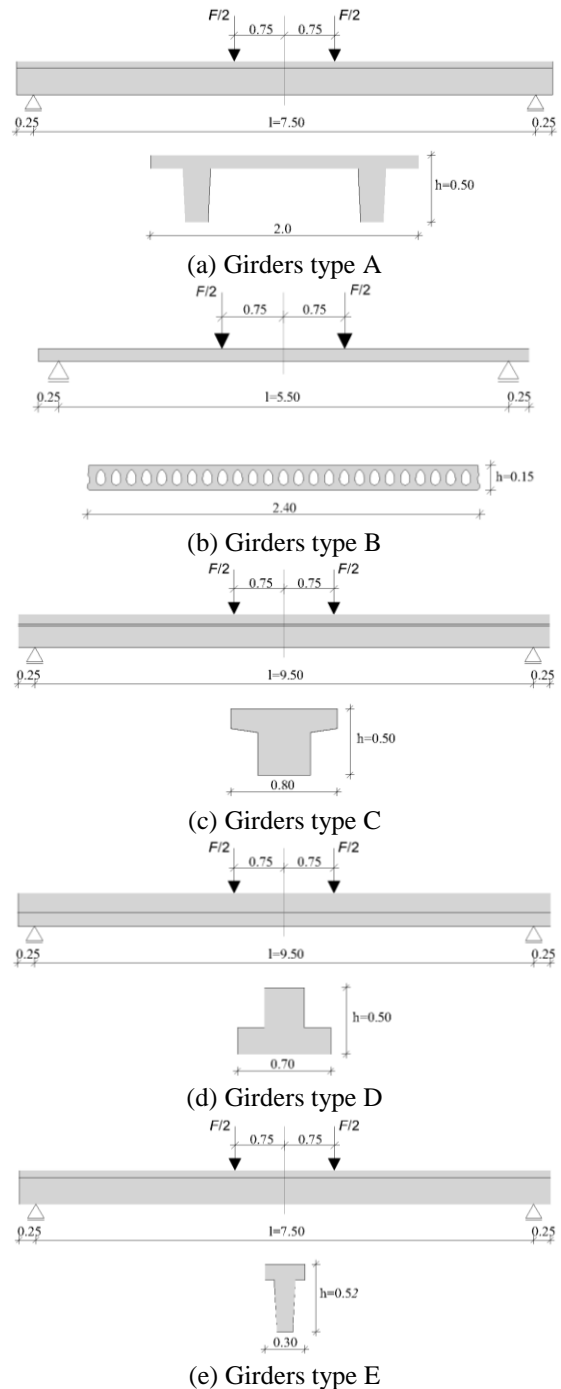


Fig. 7 Basic geometry of tested girders, Radnić *et al.* (2015)

the initial strain due prestressing, F_m is the maximum load and F_n is the load that causes ϵ_n . Part of the $F-\epsilon$ relation

Table 1 Reinforcement data and initial prestressing force for tested girders

Girder	A_p	A_s	μ_p	P_o (kN)
A1	12#3/8"	/	1.0	696
A2	8#3/8"	4Ø12	0.73	464
A3	4#3/8"	6Ø14	0.40	232
A4	/	6Ø18	0	/
B1	14#3/8"	/	1.0	812
B2	11#3/8"	17Ø6+1Ø8	0.76	638
B3	7#3/8"	18Ø8	0.54	406
B4	4#3/8"	18Ø10	0.30	232
B5	/	24Ø10	0	/
C1	10#3/8"	/	1.0	580
C2	8#3/8"	2Ø14	0.80	464
C3	5#3/8"	3Ø16	0.56	290
C4	3#3/8"	3Ø20	0.33	174
C5	/	1Ø22+2Ø25	0	/
D1	12#3/8"	/	1.0	756
D2	10#3/8"	4Ø8	0.88	630
D3	6#3/8"	4Ø16	0.53	378
D4	4#3/8"	4Ø18	0.37	252
D5	/	4Ø20+1Ø22	0	/
E1	6#3/8"	/	1.0	348
E2	4#3/8"	2Ø12	0.73	232
E3	2#3/8"	3Ø14	0.40	116
E4	/	3Ø18	0	/

over $\varepsilon > \varepsilon_m$ is not considered for the same reason as the load-displacement relation (see section 2.1). It is also clear from Eq. (3) that

$$0 \leq c_{d\varepsilon} \leq 1 \quad (4)$$

Strain ε can correspond to the strain of classical reinforcement (ε_s), concrete strain (ε_c) and strain of prestressing reinforcement (ε_p), i.e.,

$$\varepsilon = \varepsilon_s = \varepsilon_c = \varepsilon_p \quad (5)$$

Load F_n is defined as in section 2.1.

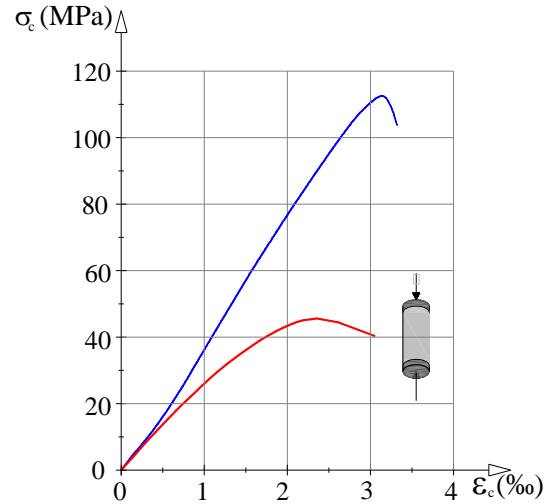
2.3 Calculation of ductility over load-curvature relation

The structure ductility index defined by load (F)-curvature (φ) relation can be calculated according to Fig. 5, analogous to those in sections 2.1 and 2.2, by

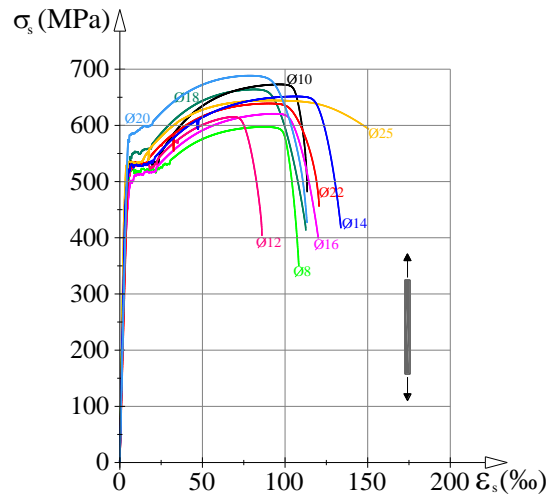
$$c_{d\varphi} = [(\varphi_m - \varphi_n)/(\varphi_m - \varphi_o)] \cdot [(F_m - F_n)/F_m] \quad (6)$$

where $c_{d\varphi}$ is the curvature ductility index, φ_m is the curvature at load F_m , and φ_n is the curvature at specified nonlinearity that is caused by load F_n . Loads F_m and F_n are the same as described in section 2.1 and 2.2. The following also applies

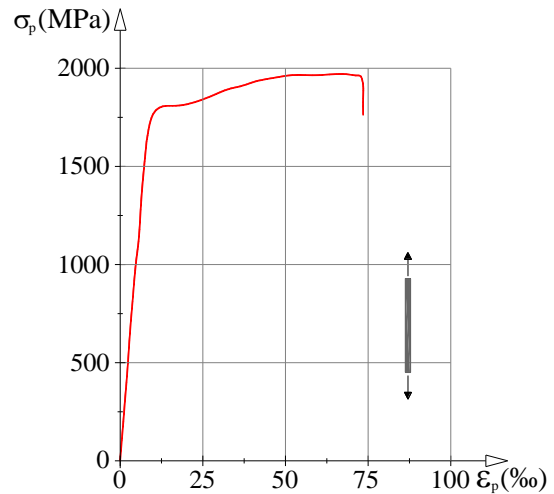
$$0 \leq c_{d\varphi} \leq 1 \quad (7)$$



(a) Concrete



(b) Classical reinforcement B



(c) Prestressed reinforcement

Fig. 8 Established stress-strain relation

Curvature is defined over cross-section curvature, as

$$\varphi = (\varepsilon_s^b + \varepsilon_c^u)/d \quad (8)$$

where ε_s^b is the strain of lower classical reinforcement in the bottom flange, ε_c^u is the concrete strain of upper edge of the

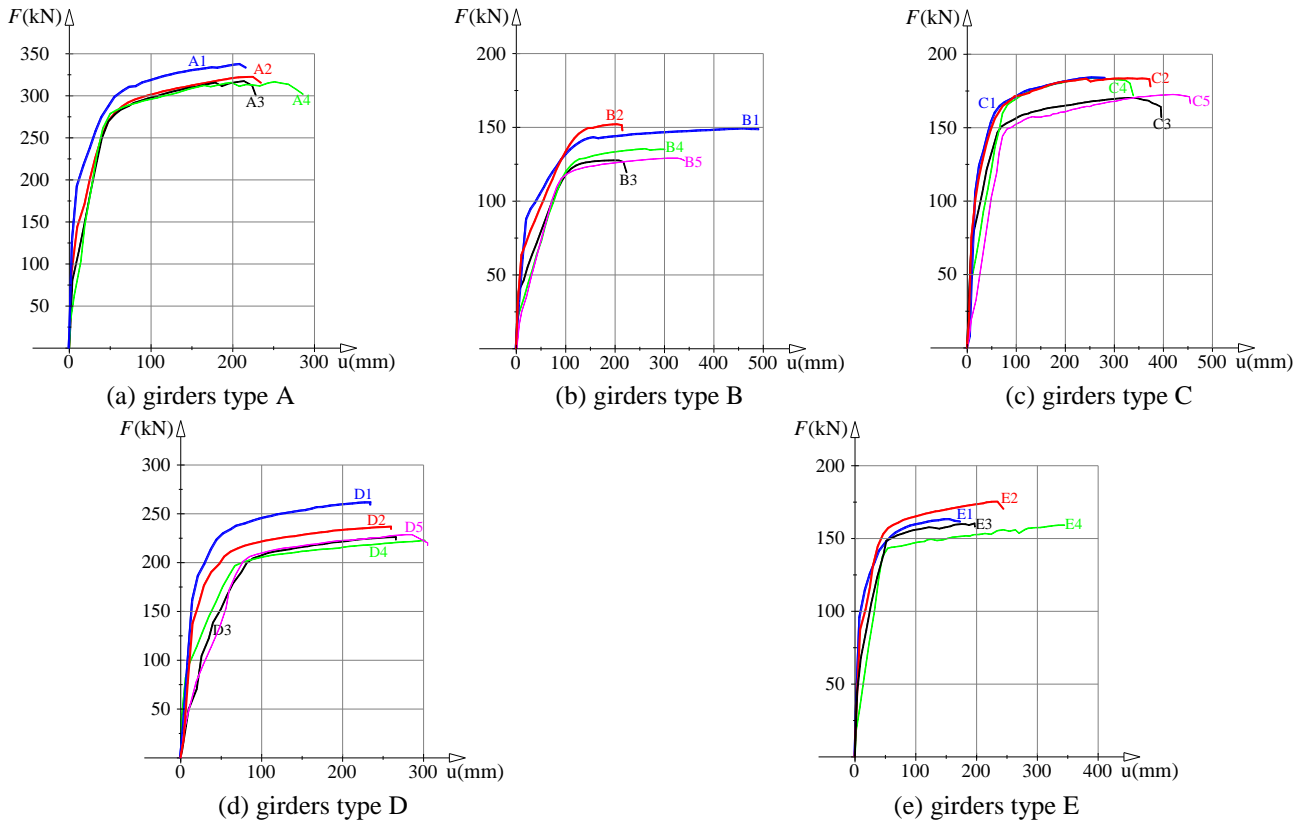


Fig. 9 Load (F)-vertical displacement in the midspan of the girders (u) relation

concrete girder and d is distance from the aforementioned locations (Fig. 6).

3. Performed experimental tests

Results from previous experiments on several large-scale concrete girders with different ratios of prestressed and classical reinforcement are briefly presented below. Radnić *et al.* (2015) provide detailed data on these tests. Prefabricated girders are widely used in practice, and their basic geometry is presented in Fig. 7. The girders are supported at the ends and loaded by force F gradually up to failure. Spans of girders were $l=5.5-9.5$ m, with height $h=0.15-0.52$ m and ratios $l/h=14.4-36.7$.

Girder types A, B and C were made by normal strength concrete class of C40/50 and girder types D, E were made by high strength concrete class of C90/105. The girders exhibited large differences in bending stiffness

All types of tested girders (A-E) had more subtypes, with different ratio of prestressed and classical reinforcement: prestressed reinforcement only, dominantly prestressed and small classical reinforcement, an equal prestressed and classical reinforcement, small prestressed and dominantly classical reinforcement, and classical reinforcement only. Total reinforcement is adopted so that all subtypes of every type of girder have an equal ultimate bearing capacity. However, some girders had small differences in ultimate bearing capacity due to deviations in such parameters as actual surface, strengths and position of

steel bars, cross-sectional geometry.

The coefficient of prestressed reinforcement μ_p is defined by

$$\mu_p = A_p/A_{\text{tot}} = A_p/(A_p + nA_s); \quad (9)$$

$$n = f_s/f_p = 650\text{MPa}/1900\text{MPa} = 0.342$$

where A_p is the area of prestressed reinforcement in the bottom belt of the girders, A_{tot} is the total area of tension reinforcement in the bottom belt of the girders, A_s is the area of the classical reinforcement in the bottom belt of the girders, f_s is the tensile strength of the classical reinforcement and f_p is the tensile strength of the prestressed reinforcement (tendons). Data of adopted reinforcement and initial prestressing force (P_0) in tendons for all tested girders are presented in Table 1.

Tendons with a diameter of 3/8" and a cross-sectional area of $A_p=52$ mm² were used in all prestressed concrete girders. A prestressed reinforcement in the Y1860S7 class strength and classical reinforcements in the B500B class strength according to Eurocode 2 (EN 1992-1-1 2004) were used. The initial tensile stress in the tendons in girders type A, B, C, E were $\sigma_{p0}=1076.4$ MPa and in girders type D were $\sigma_{p0}=1170$ MPa.

Experimentally determined stress-strain relations for classical reinforcement ($\sigma_s-\epsilon_s$), prestressed reinforcement ($\sigma_p-\epsilon_p$) and concrete in compression ($\sigma_c-\epsilon_c$) are presented in Fig. 8.

The midspan of the concrete girders were measured for each increment of load F : vertical displacements, strains of concrete on the girder's bottom and top, strain of classical

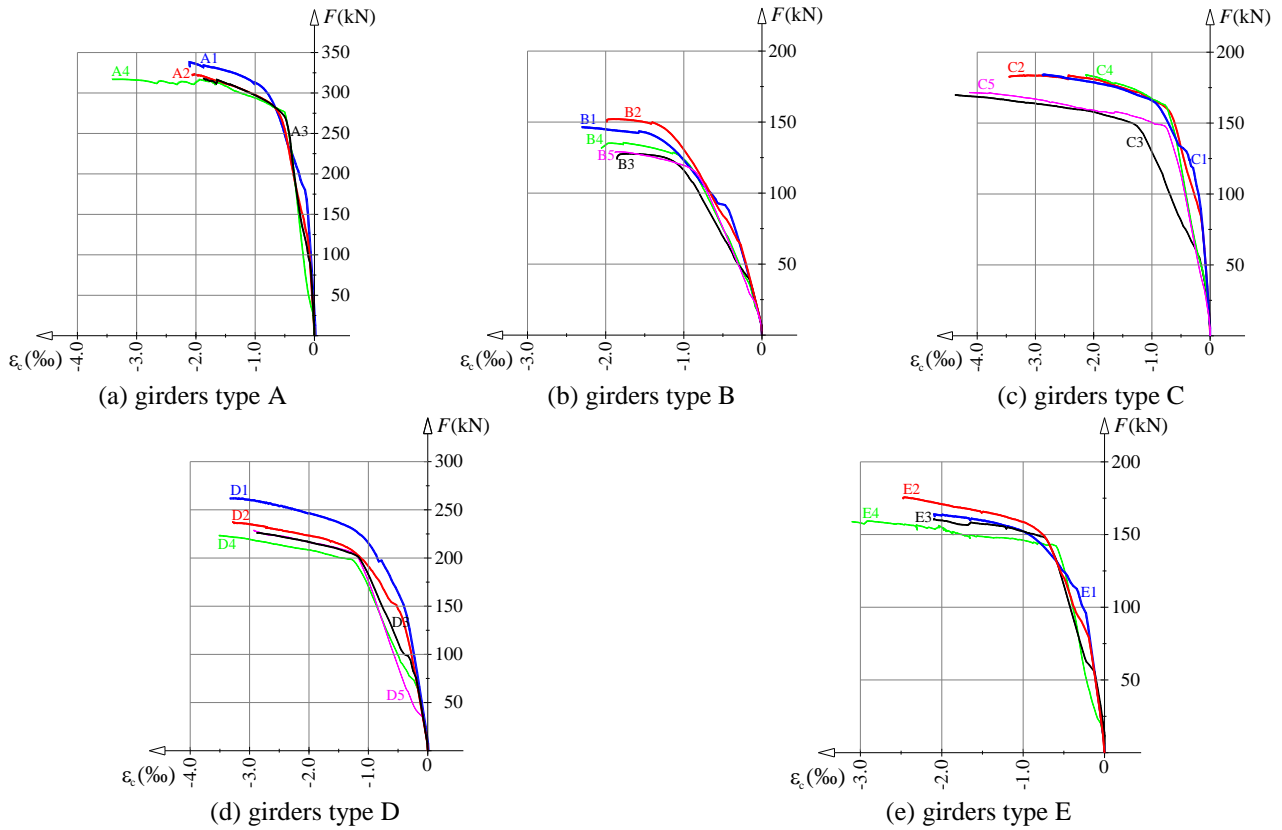


Fig. 10 Load (F)-concrete strain on the top of the girders in the midspan (ϵ_c) relation

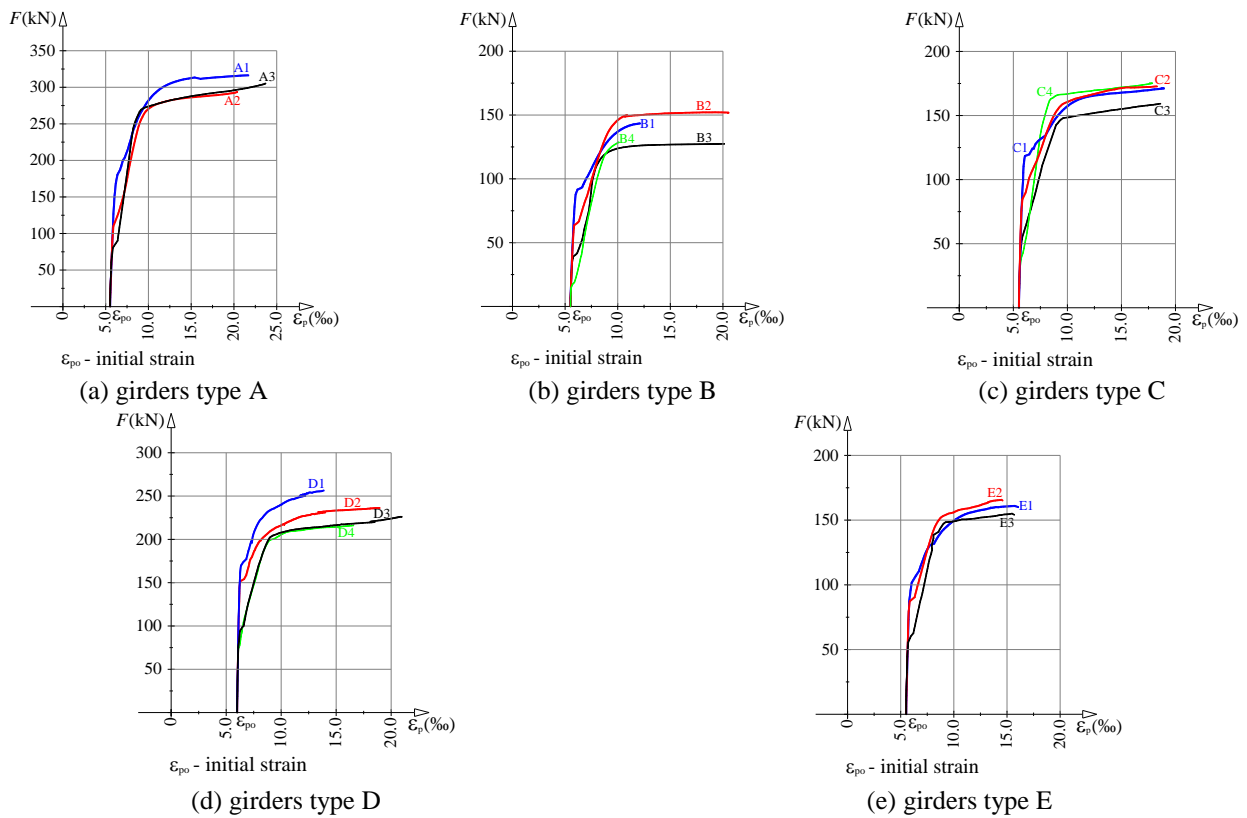


Fig. 11 Load (F)-strain of prestressed reinforcement at the bottom of the girders in the midspan (ϵ_p) relation

reinforcement on the girder's bottom and top, strain of lower tendons and width of the main crack. Some measured

results are briefly presented and discussed below.

The load (F)-vertical displacements (u) relation is

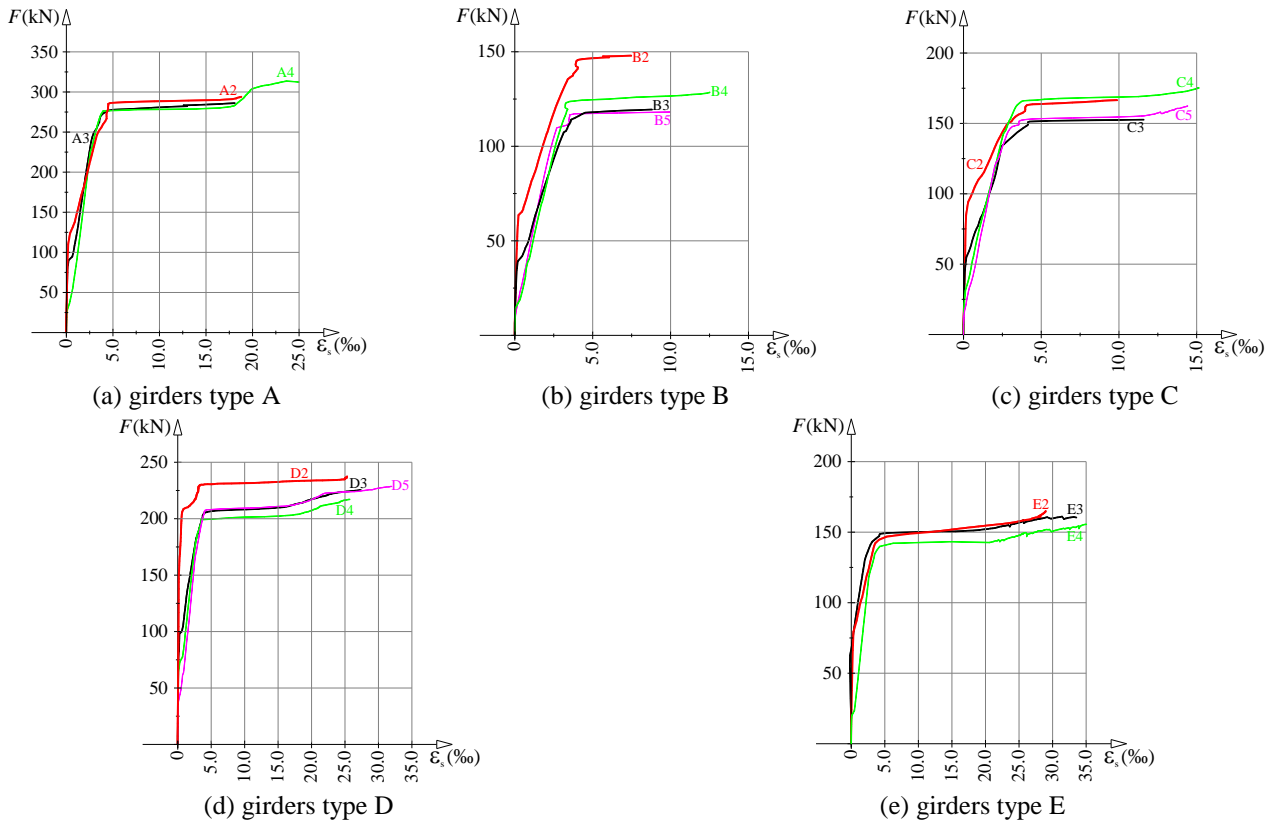


Fig. 12 Load (F)-strain of classical reinforcement at the bottom of the girders in the midspan (ϵ_s) relation

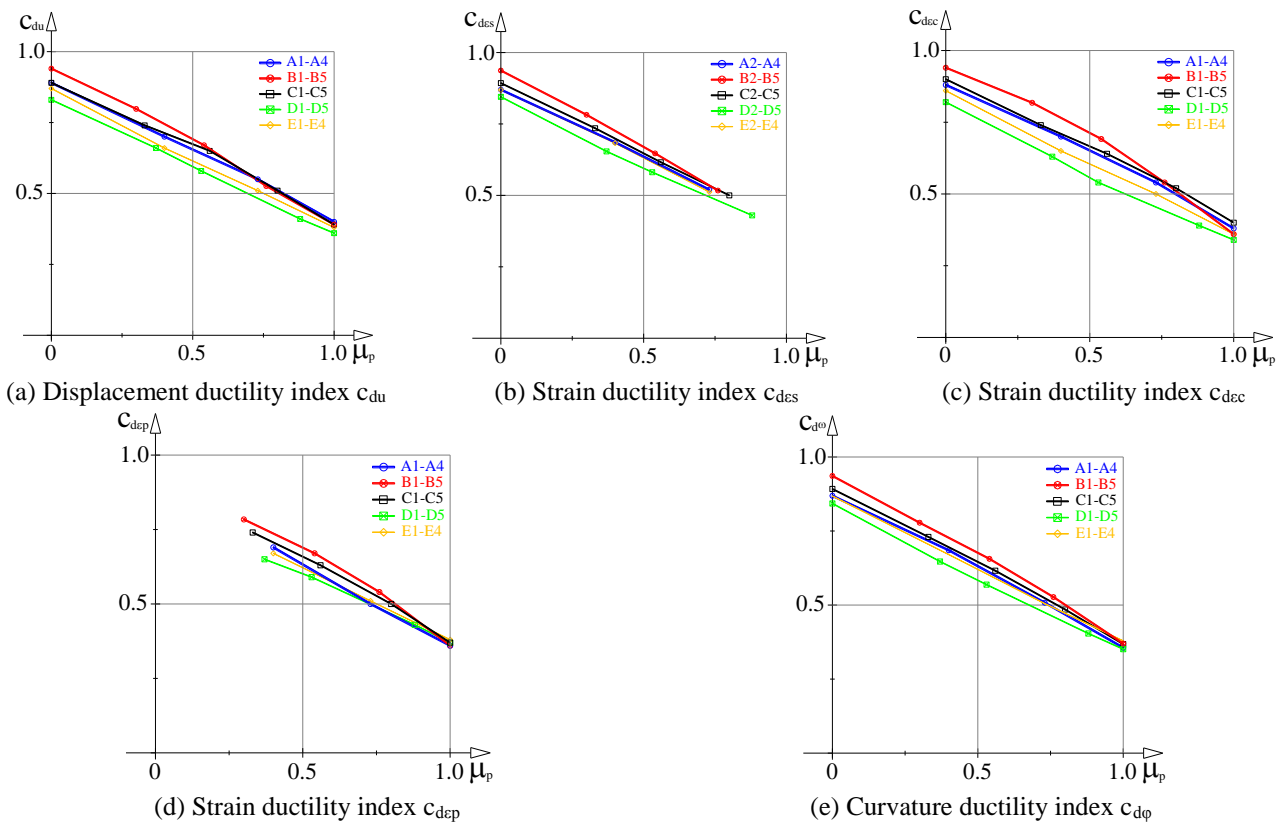


Fig. 13 Relation of displacement, strain and curvature ductility index to the ratio of prestressed reinforcement (μ_p) for $F_n = F_{cr}$

presented in Fig. 9, load (F)-concrete strain on the top of the girders (ϵ_c) relation is presented in Fig. 10, load (F)-

strain of classical reinforcement at the bottom of the girders (ϵ_s) relation is presented in Fig. 11, and load (F)-strain of

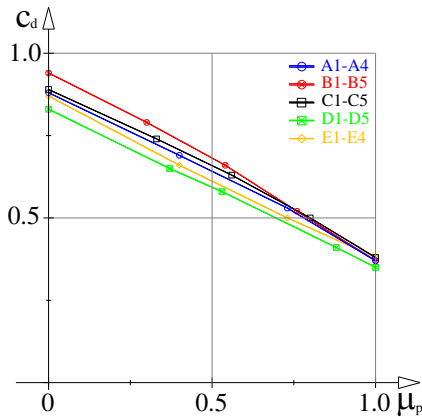


Fig. 14 Average ductility index c_d for each type of tested girders

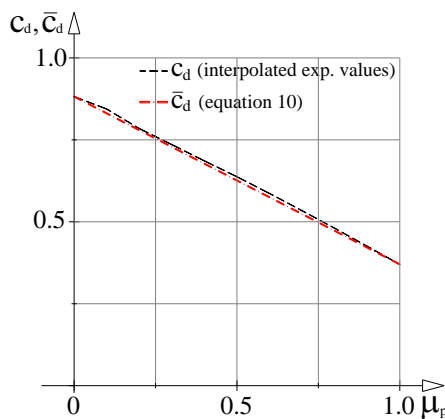


Fig. 15 Average ductility index \bar{c}_d for all tested girders

prestressed reinforcement (ϵ_p) relation is presented in Fig. 12.

All girders with prestressed reinforcement experienced camber before application of the load F , and all girders with classical reinforcement only experienced deflection. Behaviour of all concrete girders was linear-elastic before cracking of the concrete in tension. The loading value $F_n=F_{cr}$ at the moment of first cracking in concrete was especially dependent on ratio of prestressed and classical reinforcement i.e., of degree of prestressing. An increase in μ_p , resulted in increased value of F_{cr} . At the moment of concrete cracking, strains of classical reinforcement, prestressed reinforcement and compression concrete were suddenly increased. Additionally, vertical displacements of the girders were increased due to decreasing bending stiffness.

Further increases of load F , at the beginning of yielding of classical reinforcement, produced a rapid decrease of girder bending stiffness and increase of its deflection. There was also a great increase of strains in the prestressed reinforcement and in the concrete on the top of the girders. Displacements and strains significantly increased just before girder failure. Girders of the same type had increased displacement at failure after decreasing the degree of prestressing. Although tests assumed that all subtypes of concrete girders had the same load bearing capacity, a fairly large discrepancy was visible between some girders.

4. Ductility index of tested girders

On the basis of the adopted approach and presented expressions in section 2., the ductility index for tested girders presented in section 3., overall displacements, strains and curvatures are calculated according to Figs. 9-12 and presented in Fig. 13. The ductility index calculation adopted $F_n=F_{cr}$, as first nonlinearities were caused by the appearance of the first cracks in concrete i.e., exceeding of tensile strength of concrete, in all tested girders.

Displacement ductility index c_{du} is presented in Fig. 13(a), strain ductility index c_{des} (corresponds to the strain of classical tension reinforcement) in Fig. 13(b), strain ductility index c_{dec} (corresponds to the strain of concrete in compression) in Fig. 13(c), strain ductility index c_{dep} (corresponds to the strain of prestressed reinforcement) in Fig. 13(d), and curvature ductility index $c_{d\phi}$ in Fig. 13(e).

It is noticeable that all diagrams on Fig. 13(a)-13(e) are not only similar in shape, but that they also have similar ductility index. This similarity of observed ductility index is expected since the displacements, curvatures and strains are interdependent. In expressions (1), (3) and (6) for the calculation of ductility index, the second index on the right side of the expressions is taken as equal across all expressions. Ductility index are the largest for girders reinforced with classical reinforcement and smallest for girders reinforced with only prestressed reinforcement. Ductility index of prestressed girders decrease approximately linearly with an increasing coefficient of prestressed reinforcement μ_p .

From Fig. 13 it is clear that all observed ductility index depend on girder type (A, B, C, D, E). Namely, tested girders had different bending stiffness, shape of cross-section, concrete strength (modulus of elasticity), percentage of reinforcement and other characteristics. However, this difference is small and ranges up to approximately ± 7 percent of the average value.

As expected, for classically reinforced girders, type B had the maximum ductility index while type D had the minimum ductility index. Girder type B had by far the greatest span-height ratio (36.7) accompanied by a very small bending stiffness. Girder type D was made using high strength concrete, and it had a low centre of gravity of cross-section (lower tensile stresses and crack opening at higher loading), smaller span-height ratio (19) and generally the highest bending stiffness.

For prestressed concrete girders, girder type D had the minimum ductility index, which is logical. The differences between the ductility indexes for the observed girders decreased with the increasing of prestressed reinforcement. For fully prestressed girders some ductility index had similar values.

One of the parameters that affect the ductility index is the percentage of tensile reinforcement in concrete girders. For tested girders type A; B; C; D; E the percentage of tensile reinforcement (expressed via classical reinforcement) amounted to approximately 0.54; 0.52; 0.51; 0.61; 0.83. Therefore, the girders contained medium reinforcement and were expected to have a large ductility when reinforced with only classical reinforcement. In girders with a very low percentage of tensile reinforcement,

failure could appear at the occurrence of first cracks in concrete. Ductility index of such girders is equal to zero. In a case of high percentage of tensile reinforcement in girders, the girder bending stiffness increases and postpones the occurrence of the first cracks. Those girders will have a small ductility index.

From an engineering standpoint, it can be said that the displacement and curvature ductility index are more acceptable than the strain ductility index. Namely, girder displacements and curvatures could be easily observed during the increase of loading, while the strains in materials of girder are visually hidden. However, if we take all observed ductility index c_{du} , c_{des} , c_{dec} , c_{dep} , c_{dep} for each type of tested girders as equally measurable and calculate the average value, then we can declare it as an average ductility index or just ductility index. Calculated values of c_d for different tested girders are presented in Fig. 14, where their small differences are visible.

The average value of ductility index c_d between all girder types A,B,C,D,E in Fig. 14 can be calculated using linear interpolation at discrete points of each girder's subtypes, marked as c_d and graphically presented on Fig. 15 (continuous line).

The resulting curve can be approximated by line equation, as

$$\bar{c}_d = 0.882 - 0.512\mu_p \quad (10)$$

and also graphically presented on Fig. 15 (dashed line). Expression (10) can be used for calculation of ductility index of classically and prestressed concrete girders in practice, under condition that the girders characteristics (e.g., bending stiffness, mechanical properties of concrete, percentage and mechanical properties of reinforcement, and cross-sectional shape) are similar to the tested girders presented in section 3.

5. Conclusions

The paper initially presented one approach in addition to expressions for the calculation of ductility index of classically reinforced and prestressed concrete girders subjected to short term static load. Ductility index are defined based on displacement (displacement ductility index), curvature (curvature ductility index) and strains in concrete, classical and prestressed reinforcement (strain ductility index). Expressions for ductility index are the product of two influences: (i) the remaining displacements (curvatures, strains) after the appearance of the specified nonlinearities in the girder in relation to the total displacements (curvatures, strains) at reaching the maximum girder bearing capacity, (ii) the remaining load after specified nonlinearities in the girder in relation to the maximum load at girder failure. Ductility index defined with this approach are in the range of zero to one (0-1). The ductility index equal to zero corresponds to the girders lacking nonlinearities just before failure (so-called brittle collapse). Ductility index equal to one correspond to the girders where nonlinearities have begun to appear at the beginning of the loading.

Proposed expressions for the calculation of ductility index were applied to the results of performed static experimental tests of five different types of large-scale concrete girders with different ratios of prestressed and classical reinforcement. This study showed that displacement ductility index, curvature ductility index and strain ductility index differ slightly. This is logical because displacements, curvatures and strains are connected and interdependent and the second member in the expressions for calculation of ductility index will always be equal. The average ductility index is introduced and calculated as the average value of displacement ductility index, curvature ductility index and strain ductility index.

Ductility index of prestressed girders decrease approximately linearly with increasing coefficient of prestressed reinforcement μ_p . Such factors as bending stiffness, shape of cross-section, concrete strength, and percentage of reinforcement influence ductility index. Based on previous analyses, an expression for the calculation of average ductility index or just ductility index of classically reinforced and prestressed concrete girders is suggested.

This expression can only be used for girders in practice that are similar to the tested girders.

According to the proposed approach, the value of the ductility factor always ranges between 0 (without ductility) and 1 (ideal ductile structures with nonlinear load-displacement relation in all range of load action up to structure collapse), what is practical and easy to remember. Ductility index were defined over multiple structural parameters (displacement, curvature and strains of all materials). The analysed examples shows that the value of ductility index across all parameters was very close, which was expected and confirmation of the appropriate approach, because considered parameters were interrelated for all structures.

In accordance with the proposed approach and author's experience in the design (calculation) and realisation of concrete structures in practice, we consider that for classically reinforced concrete elements average ductility index should be $\bar{C}_d \geq 0.6$ and for full-prestressed ($\mu_p=1$) should be $\bar{C}_d \geq 0.3$.

References

- Abdelrahman, A.A., Tadro, G. and Rozkalla, S.H. (1995), "Test model for the first Canadian smart highway bridge", *ACI Struct. J.*, **92**(4), 451-458. <https://10.1.1.469.2167&rep=rep1&type=pdf>.
- Arslan, M.H. (2012), "Estimation of curvature and displacement ductility in reinforced concrete buildings", *KSCE J. Civil Eng.*, **16**(5), 759-770. <https://doi.org/10.1007/s12205-012-0958-1>.
- Bouزيد, H. and Kassoul, A. (2016), "Curvature ductility of high strength concrete beams according to Eurocode 2", *Struct. Eng. Mech.*, **58**(1), 1-19. <https://doi.org/10.12989/sem.2016.58.1.001>.
- Chen, X.C., Bai, Z.Z. and Au, F.T.K. (2017), "Effect of confinement on flexural ductility design of concrete beams", *Comput. Concrete*, **20**(2), 129-143. <https://doi.org/10.12989/cac.2017.20.2.129>.
- Dolan, C.W., Hamilton, III, H.R., Bakis, C.E. and Nanni, A. (2001), *Design Recommendations for Concrete Structures*

- Prestressed with FRP Tendons*, FHEA Contract (DTFH61-96-c-00019) Final Report.
- European Committee for Standardization (CEN) (2004), *Eurocode 2: Design of Concrete Structures-Part 1: General Rules and Rules for Buildings*, EN 1992-1-1:2004, Brussels, Belgium.
- Ghallab, A. (2014), "Ductility of externally prestressed continuous concrete beams", *KSCE J. Civil Eng.*, **18**(2), 595-606. <https://doi.org/10.1007/s12205-014-0443-0>.
- Grace, N.F., Soliman, A.K., Abdul-Sayed, G. and Saleh, K.R. (1998), "Behaviour and ductility of simple and continuous FRP reinforced beams", *J. Compos. Constr.*, **2**(4), 186-194. [https://doi.org/10.1061/\(ASCE\)1090-0268\(1998\)2:4\(186\)](https://doi.org/10.1061/(ASCE)1090-0268(1998)2:4(186)).
- Hofstetter, G. and Mang, H.A. (1996), "Computational plasticity of reinforced and prestressed concrete structures", *Comput. Mech.*, **17**(4), 242-254. <https://doi.org/10.1007/BF00364827>.
- Marí, A.R., Oller, E. and Bairán, J.M. (2011), "Predicting the response of FRP-strengthened reinforced-concrete flexural members with nonlinear evolutive analysis models", *J. Compos. Constr.*, **15**(5), 799-809. <https://doi.org/10.1007/BF00364827>.
- Naaman, A.E. and Jeong, S.M. (1995), "Structural ductility of concrete beams prestressed with FRP tendons", *Proceeding of the 2nd International RILEM Symposium*, London, U.K.
- Pam, H.J., Kwan, A.K.H. and Ho, J.C.M. (2001), "Post-peak behavior and flexural ductility of doubly reinforced normal- and high-strength concrete beams", *Struct. Eng. Mech.*, **12**(5), 459-474. <https://doi.org/10.12989/sem.2001.12.5.459>.
- Park, R. (1989), "Evaluation of ductility of structures and structural assemblages from laboratory testing", *Bullet. New Zealand Nat. Soc. Earthq. Eng.*, **22**(3), 155-166.
- Park, R. and Paulay, T. (1975), *Reinforced Structures*, John Wiley & Sons, Canada.
- Pisanty, A. and Regan, P.E. (1998), "Ductility requirements for redistribution of moments in reinforced concrete elements and possible size effect", *Mater. Struct.*, **31**(8), 530-535. <https://doi.org/10.1007/BF02481534>.
- Radnić, J., Markić, R., Glibić, M., Čubela, D. and Grgić, N. (2015), "Experimental testing of concrete beams with different levels of prestressing", *J. Mater. Des. Appl.*, **230**(3), 760-779. <https://doi.org/10.1177/1464420715585069>.
- Spadea, G., Bencardino, F. and Swamy, R.N. (1997), "Strengthening and upgrading structures with bonded CFRP sheets design aspects for structural integrity", *Proceedings of the 3rd International RILEM Symposium on Non-Metallic (FRP) for Concrete Structures*, Sapporo, Japan.
- Tan, D.B., Delpak, R. and Davies, P. (2005), "Ductility and deformability of fibre-reinforced polymer strengthened reinforced beams", *Proceedings of the Institution of Civil Engineers: Structures and Buildings*, **157**(1), 19-30. <https://doi.org/10.1680/stbu.2004.157.1.19>.
- Thomsen, H.H., Spacone, E., Limkatangu, S. and Camata, G. (2004), "Failure mode analysis of reinforced concrete beams strengthened in flexure with externally bonded fibre-reinforced polymers", *J. Compos. Constr.*, **8**(2), 123-131. [https://doi.org/10.1061/\(ASCE\)1090-0268\(2004\)8:2\(123\)](https://doi.org/10.1061/(ASCE)1090-0268(2004)8:2(123)).
- Young, I.Y., Park, H.G., Kim, S.S., Kim, J.H. and Kim, Y.G. (2008), "On the ductility of high strength concrete beams", *Int. J. Concrete Struct. Mater.*, **2**(2), 115-122. <https://doi.org/10.4334/IJCSM.2008.2.2.115>.
- Zou, P.X.W. (2003), "Flexural behaviour and deformability of fiber reinforced polymer prestressed concrete beams", *J. Compos. Constr.*, **7**(4), 275-284. [https://doi.org/10.1061/\(ASCE\)1090-0268\(2003\)7:4\(275\)](https://doi.org/10.1061/(ASCE)1090-0268(2003)7:4(275)).